Secular variability in the large-scale baroclinic transport of the North Pacific from 1950–1970

by Warren B. White[1]

ABSTRACT

A time sequence of meridional baroclinic transport (0/1000 db) across the Subtropical gyre of the North Pacific is constructed, based upon available hydrographic data collected from 1950–1970. This time sequence displays significant variability, with a maximum possible range ±25% about the long-term mean and a principal time scale of approximately six years. A comparison of this time sequence with that of the Kuroshio (Nitani, 1972) shows good correlation in both amplitude and phase. These time sequences show that from 1955–58 and from 1963–68, the baroclinic transport of the Subtropical gyre was larger than normal, being smaller from 1959–1962. Upon mapping the transport function over the entire North Pacific for these three time periods, the morphology in the western part of the Subtropical gyre changed significantly, tending to contract during years of large transport, and to expand in years of weak transport. In the eastern part of the subtropical gyre little change in morphology occurred between these time periods.

The principal time scale of variability, being approximately six years, is on the same scale as that for significant baroclinic response of a two-layer ocean to transient winds (Veronis and Stommel, 1956). Therefore, the time sequence is compared with a similar one of the theoretical geostrophic transport taken from the routine computations of Fofonoff (1963) and Wickett (1971), both based upon Sverdrup's (1947) theory. Between the observed and theoretical time sequences no correlation exists, the theoretical time sequence being essentially uniform at the six year time scale. Possible reasons for this disagreement are discussed.

In computing the observed baroclinic transport time sequence, the local baroclinic eddy field presented a serious space/time aliasing problem. Based on the recent work of Bernstein and White (1974) on the statistics of this eddy field, an appropriate low pass filter could be designed that effectively reduced this source of contamination, allowing the longer period fluctuations to be seen.

1. Introduction

In recent years, the study of how the ocean and atmosphere interact to produce large-scale changes in climate has become more popular (Namias, 1968). Recent work of Vondar Harr and Oort (1973) suggests that the role of poleward transport of heat by the ocean is an important element in this. This is manifested in the observation that the western North Pacific north of 30N is a region of annual surface heat loss (Wyrtki, 1965), most of this occurring in the autumn and winter months. To replace

1. Scripps Institution of Oceanography, University of California, P.O. Box 1529, La Jolla, California, 92037, U.S.A.

this heat loss, the Kuroshio is thought to advect heat into the region from the equatorial North Pacific. It is of immense interest to learn what role the fluctuating component of the Kuroshio has upon the thermal structure in this part of the ocean. This could conceivably have an important effect upon the winter climate of the Northern Hemisphere.

And yet, little is known about how the transport of the Kuroshio fluctuates. Only recently, baroclinic transport variability in the Kuroshio system has been studied by Nitani (1972), who has constructed 10 year time sequences of baroclinic transport (0/1000 db) across the stream at a number of locations and found secular fluctuation of up to $\pm 25\%$ of the long-term mean, lasting for several years. Yet he is hesitant to ascribe reality to the phase of the secular fluctuations because of the inherent problems in defining the boundaries of the Kuroshio and resolving the possible space/time aliasing.

In the present study, the large-scale transport variability suggested by Nitani is supported and put in perspective with a more expanded investigation of the baroclinic transport fluctuations in the Subtropical gyre. Initially, only one time sequence of baroclinic transport is considered; between the coast of Baja California and the middle of the Subtropical gyre off the east coast of Asia. This record is compared to that of the Kuroshio transport in an attempt to support fluctuations in the latter by the obvious connection between the interior flow and that of the western boundary. The apparent agreement between these two time sequences indicates that over certain periods of years the transport of the Kuroshio and the Subtropical gyre was altered considerably. This is further supported by constructing horizontal maps of transport function, allowing an investigation into changes in the morphology of the gyre accompanying the secular change in baroclinic transport.

Because the hydrographic data are sparsely distributed in both time and space, careful attention is given to the aliasing problems that this data distribution entails. This leads to a pertinent discussion concerning the importance of spatial filtering the influence of the highly energetic baroclinic eddies that are found throughout the North Pacific (Bernstein and White, 1974).

2. Source of hydrographic data

Upon request, the Natioaal Oceanographic Data Center sorted by year, season and 2 degree squares all of the hydrographic station data (extending deeper than 250 m) taken in the North Pacific from 1950 to the present. The position of these hydrographic stations were plotted on individual seasonal maps of the North Pacific, from which most of the hydrographic stations were found to be sparsely distributed away from the continental margins, except in the vicinity of the Hawaiian Islands and the ocean weather stations. Furthermore, most hydrographic stations were taken in the summer months (defined as July, August, September) with fewest in the winter months (January, February, March). Therefore, only data at positions of

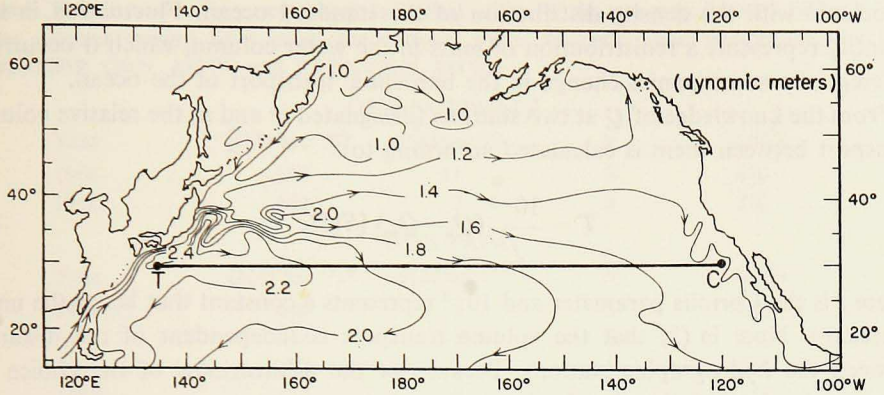

Figure 1. Location of the transport section used in this study, referenced to the mean surface flow over the North Pacific as inferred from the geopotential height anomaly taken from Reid (1961).

large concentration were useful for this study, and generally only for the summer months.

The time sequence of meridional baroclinic transport of the Subtropical gyre is determined from hydrographic stations taken at 30N, 120W off the coast of Baja California and at OWS TANGO (29N, 135E) off the east coast of Asia, both locations chosen because of the relatively high density of stations there. Much of the data off the coast of Baja California was collected as a part of the California Cooperative Fisheries Investigation based at Scripps Institution. The data of OWS TANGO was collected principally by the Japanese; from 1964–1970 as part of the Cooperative Study of the Kuroshio.

The relative position of this section is displayed in Fig. 1, together with the mean dynamic topography of the sea surface (Reid, 1961), outlining the surface morphology of the Subtropical gyre.

3. Procedure

The procedure to compute the baroclinic geostrophic transport between hydrographic stations begins by calculating the transport function Q (Sverdrup, et al, 1943), page 463) at each station:

$$Q = \int_0^h \Delta D \, dz \ [\mathrm{m^3 sec^{-2}}] \tag{1}$$

where ΔD is the dynamic height anomaly ($\mathrm{m^2 sec^{-2}}$) as a function of depth (0/1000 m) and h is the depth of the reference pressure surface, 1000 db in the present study. The dynamic height anomaly was calculated at standard depths by the National Oceanographic Data Center as a routine product.

The function ϱQ, where ϱ is the mean density of the ocean, represents the potential energy anomaly per unit horizontal area, or the excess potential energy above that

associated with the density distribution of the standard ocean. Fluctuation in this quantity represents a redistribution of mass in the water column, which if occurring differentially accompanies change in the baroclinic transport of the ocean.

From the knowledge of Q at two stations (designated m and n) the relative volume transport between them is calculated according to:

$$T = \frac{10^{-5}}{f}(Q_n - Q_m)\ [Sv]^*, \tag{2}$$

where f is the Coriolis parameter and 10^{-5} represents a constant that keeps the units consistant. Note in (2) that the volume transport is independent of the distance between the hydrographic stations. Because of the arbitrariness of the choice of reference level (1000 db), the absolute value of the transport measurements may or may not be taken as definitive. What is definitive are the secular fluctuations in the transport about the long-term mean. Concerning the error in transport from those in temperature and salinity incurred during the field measurements, the error analysis of Wooster and Taft (1958) was extended, with Q (0/1000 db) having a standard error of 20 $m^3 sec^{-2}$, corresponding to a standard error in transport between any two stations of .5 Sv at 30N.

4. Temporal aliasing

In the 2 degree squares around the locations of interest (29N, 135E and 30N, 120W), data sampling in time is at infrequent intervals at best. As a result, only one or two stations (if any) are available to compute an individual seasonal mean at either of these two locations. Therefore, taking the seasonal mean as representative is possible only if the aliasing from the time periods less than a season is small compared to year to year variability. As we shall see next, this cannot be shown.

At the two locations of interest, and indeed over most of the open ocean, the determination of the magnitude of temporal aliasing at the sub-seasonal level is prohibited by the absence of sequential hydrographic taken at a point throughout the season. The only place that stations have been taken with any regularity is at ocean weather stations PAPA (50N, 145W) and NOVEMBER (30N, 140W). At these locations the individual seasonal mean and variance estimates of Q have been calculated by the National Oceanographic Data Center for all seasons containing three or more hydrographic casts (at least one in each month of the season). These statistics are in Table I, along with the percent dispersion ($\pm 2\sigma/Q$) of the individual values about the seasonal mean.

In Table I, the largest percent dispersion of the individual values about the temporal mean is approximately $\pm 4\%$. Comparing the maximum dispersion at each of the two locations represented, little difference can be found. This suggests that a typical dispersion value over the entire ocean may not exceed $\pm 5\%$. This statement

* 1 Sverdrup (So) = $10^6\ m^3\ sec^{-1}$.

Table I. The dispersion (in percent) that individual values of the transport function (taken within the summer season) have about the seasonal mean, at both ocean weather stations NOVEMBER (30N, 140W) and PAPA (50N, 145W).

OWS NOVEMBER

Year	$\bar{Q}(M^3\text{sec}^{-2})$*	$\sigma(M^3\text{sec}^{-2})$	N	$(2\sigma/\bar{Q})$
1966.....	595	11	3	4%
1968.....	609	7	3	2%

OWS PAPA

Year	$\bar{Q}(M^3\text{sec}^{-2})$*	$\sigma(M^3\text{sec}^{-2})$	N	$(2\sigma/\bar{Q})$
1959.....	450	5	5	2%
1961.....	434	5	8	2%
1965.....	460	5	8	2%
1966.....	454	2	7	1%

* Relative to 1000 db.

awaits additional confirmation, but it is utilized for the present. Therefore, time sequences spanning twenty years, yet consisting of individual values of Q taken within each individual season, must display a greater than 10% variability from year to year necessary for this variability to be statistically significant at about the 90% confidence level. More importantly, upon considering the differences in transport function between the two stations of interest here, where $\Delta\bar{Q}$ is typically 300 m^3sec^{-2}, this level of uncertainty is even more restrictive, being approximately $\pm 10\%$ of the mean $\Delta\bar{Q}$.

5. Spatial aliasing

In the foregoing discussion, the intraseasonal dispersion about the individual seasonal mean, Q, was less than $\pm 5\%$ of the mean. A potentially more important aliasing arises from the local spatial variability, due to the presence of the baroclinic eddy field in the central North Pacific (Bernstein and White, 1974).

In this latter work, the central North Pacific was found to be overlain with a mosaic of baroclinic eddies, with length scales (i.e., one half wavelength) ranging from 50 km to 250 km, with the amplitude of the eddies directly proportional to the length scale. In addition, the larger eddies were found to have transport magnitudes (0/1000 db) that were on the same order as the transport of the entire Subtropical gyre. This indicates that the presence or absence of a 250 km diameter eddy at one end of a zonal section could seriously contaminate a large-scale transport calculation across the section.

A more accurate measure of this local spatial variability is obtained by computing the variance (σ^2) about a spatial mean $\bar{Q}$ taken over a 5 degree square of ocean. This was done in the vicinity of the two ocean weather stations, PAPA and NOVEMBER, utilizing data that was nearly randomly distributed throughout the 5 degree squares. These statistics are in Table II, along with the percent dispersion ($\pm 2\sigma/\bar{Q}$) of the indivudual values about the spatial mean transport function.

Table II. The dispersion (in percent) that individual values of the transport function (taken over a 5 degree square of ocean) have about the spatial mean, at both ocean weather stations NOVEMBER (30N, 140W) and PAPA (50N, 145W).

OWS NOVEMBER

Year	$\bar{Q}(M^3sec^{-2})$*	$\sigma(M^3sec^{-2})$	N	$(2\sigma/\bar{Q})$
1965.....	598	14	12	5%
1966.....	621	18	17	6%
1967.....	594	5	22	2%
1968.....	605	11	33	4%
1969.....	598	21	13	7%

OWS PAPA

Year	$\bar{Q}(M^3sec^{-2})$*	$\sigma(M^3sec^{-2})$	N	$(2\sigma/\bar{Q})$
1956.....	447	17	5	8%
1958.....	456	12	7	5%
1965.....	463	9	14	4%
1966.....	461	12	12	5%

* Relative to 1000 db.

From Table II, the largest percent dispersion of the individual values about the spatial mean is approximately $\pm 8\%$. There seems to be little difference in the maximum dispersion at the two widely spaced weather stations, suggesting that a typical dispersion value over the entire ocean may not exceed $\pm 10\%$. Therefore, the difference in Q (or potential energy anomaly) across a 500 km eddy wavelength (i.e., 100 m^3sec^{-2}) may approach but probably does not exceed 20% of the mean potential energy anomaly of the 5 degree square. However, this is nearly as large as the difference between Q on one side of the ocean and that on the other (~ 300 m^3sec^{-2}); thus presenting an aliasing problem that is a serious source of contamination.

6. Solution to space/time aliasing problem

The work of Bernstein and White (1974) suggests that the temporal aliasing may be primarily a manifestation of the local spatial variability induced by the propagation of the local baroclinic eddy field past a fixed position in the ocean. They found in the east central North Pacific near 26N that the larger (500 km wavelength) and most energetic baroclinic eddies propagated to the west at a speed of approximately 3 cm sec^{-1} above the speed of the mean flnw. The ocean weather stations themselves are located in regions of small ambient flow; therefore, the eddies might be expected to travel by at about 3 ± 1 cm sec^{-1}. At this speed, a 500 km wave could travel 250 km during a season. Therefore, the maximum temporal variability over that three month perind might be expected to be from 1 to ½ of that possible over a 500 km wave length; and indeed, the maximum temporal variability that is observed (see Table I) over the three month period is half that of the maximum local spatial variability (i.e., $\pm 8\%$).

On the basis of past methods of sampling the marine environment, generally only one station per season is found at any one location. As such, temporal aliasing is unavoidable. Yet, the possibility that temporal aliasing is simply a manifestation of the local spatial aliasing, i.e., it arises from the propagation of the baroclinic eddy field past a fixed point, provides an alternate method of filtering, in space rather than time.

Generally, when hydrographic casts are made, they are accompanied by adjacent casts at approximately one degree intervals. These randomly sample the local baroclinic eddy field, making it possible for a spatial average that filters out the influence of the baroclinic eddies. However, to do this effectively, the length scale over which the filtering process extends should be as large as the longest wave that is creating the aliasing problem. In the wavenumber spectra for baroclinic eddies found in the central North Pacific by Bernstein and White (1975), the variance from 100 km out to 500 km increases, but falls off thereafter, suggesting the existence of a spectral gap between the variance associated with waves of 500 km and those at much larger wavelengths (i.e., those representing spatial fluctuations in the gyre itself). Therefore, a spatial average over a 500 km (5 degree) square should filter out most of the variability associated with the local eddy field and allow fluctuations in the baroclinic structure of the gyre itself to be visible.

7. Secular variability in the transport function

In this section the secular variability in the spatially averaged transport functions at two locations from 1950–1970 is considered. The locations are 135E and 120W at 30N. In the next section the meridional baroclinic transport across this zonal section is considered.

The time sequence of $\bar{Q}$ at OWS TANGO (29N, 135E) is in the upper panel of Fig. 2. As discussed in the previous section, the individual seasonal values represent a spatial mean over a 5 degree square about the central position. The error bars represent the standard error. The number below each point is the number of stations used to compute the mean and the standard error. From normal statistical procedures, the difference between any two sample means on the graph represents a significant difference (at about the 90 % con-

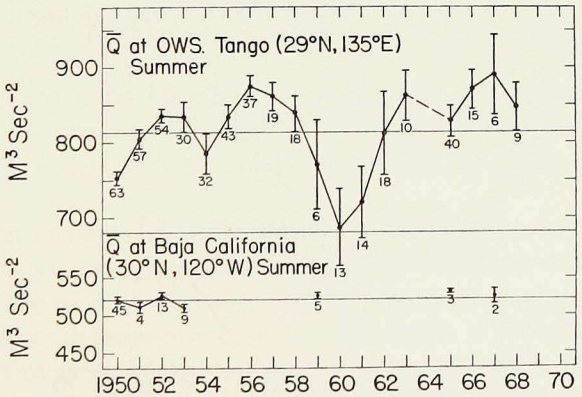

Figure 2. Time sequences of the mean transport function at OWS TANGO and off the coast of Baja California using data taken only during the summer.

fidence level) in the respective population means if their difference is greater than approximately two times the averaged standard error.

In the upper panel of Fig. 2, a strong secular variability exists, $\bar{Q}$ being above normal in 1952–1953, 1955–1958, and from 1963–1968, being below normal the other times. Generally, variability from one year to the next is not significant, but sample means at two or three year separations can be significantly different, particularly from 1956 to 1963. Percentwise, the maximum range of variability over the twenty year period is approximately $\pm 12\%$ of the mean, about equal to the maximum range of variability expected ($\pm 10\%$) from the spatial variability induced by the local baroclinic eddy field. This underscores the importance of filtering the influence of these eddies.

In the lower panel of Fig. 2 is the time sequence of $\bar{Q}$ at 30N, 12OW off the coast of Baja Califnrnia. The most noticeable aspect of this graph, other than the paucity of data, is the singular lack of any large secular variability. Percentwise, the maximum range of variability of the data available is approximately $\pm 1\%$ of the mean, clearly a tenth as large as the secular variability found in the western North Pacific.

8. Secular variability in baroclinic transport of the subtropical gyre

The baroclinic transport across the Subtropical gyre is computed by substituting the values of Q in Fig. 2 into (2). Because the secular variability at OWS TANGO is so much larger than that off the coast of Baja California, and because the former time sequence is so much more complete than the latter, the transport is computed utilizing the long-term mean value of $\bar{Q}$ off the coast of Baja California. The subsequence time sequence is in the upper panel of Fig. 3.

In this time sequence the same qualitative variability as in the potential energy anomaly at OWS TANGO is found. The long-term mean is 40 Sv, with the maximum range of variability being approximately $\pm 25\%$ of the mean. Clearly this variability is very large and could have an important effect upon the variability of heat transport in the ocean.

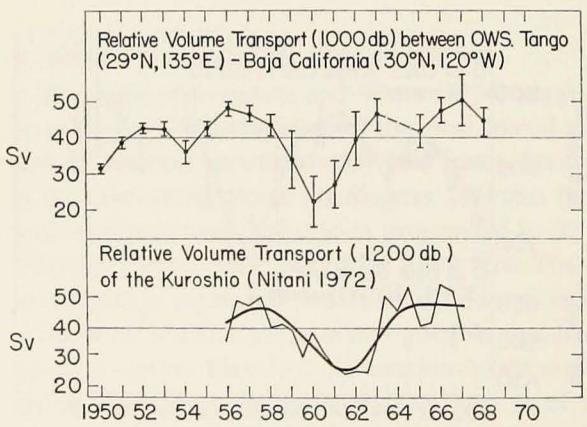

Figure 3. Time sequence of the mean meridional baroclinic transport (0/1000 db) across the Subtropical gyre, together with that of the Kuroshio (Nitani, 1972).

To support this secular variability, it is compared with that found in the time sequence of baroclinic transport of the Kuroshio (Nitani, 1972) southeast of Yakushima

Island (lower panel of Fig. 3); the latter a measure of the baroclinic transport between the Japanese islands and the Ryukyu islands, a channel through which the Kuroshio flows. Both time sequences have a long-term mean transport of 40 Sv, each displaying a maximum range of variability of $\pm 25\%$ of the mean. The secular variability from 1956 to 1968 is present in both, with the transport of the Subtropical gyre seeming to lead in phase the transport of the Kuroshio by one or two years. However, the apparent phase difference is vague, made so by the standard error in the upper time sequence that precludes a clear resolution of peaks and troughs.

9. Secular changes in the morphology of the subtropical gyre

The foregoing time sequence of baroclinic transport indicates that the maximum transport of the Subtropical gyre was much weaker (by nearly 50%) over the time period 1959–62, than over the other two time periods 1955–58 and 1963–68. It is important to see if this is a general feature of the gyre, independent of the two locations used in the transport computation. Moreover, it is of interest to map some of the more outstanding changes in morphology of the gyre between these periods of high and low transpnrt.

To accomplish this end, we have computed the average transport function (together with the standard error) at each 5 degree square over the North Pacific from all of the hydrographic data taken within these three time periods. These averaged data are mapped and contoured in Fig. 4a, b and c, together with the associated error maps.

Comparing the $\bar{Q}$ maps for 1955–58 and 1963–68 (periods of high baroclinic transport) with that for 1959–62 (a period of low baroclinic transport), one finds that in the vicinity of OWS TANGO a meander exists in the Kurnshio during the latter time period that does not exist in the former two periods. This would have the effect of making the $\bar{Q}$ function at OWS TANGO much smaller than it would otherwise be during the period 1959–62. Yet, the maximum transport of the gyre is still much lower during this time period (i.e., 1959–62) than in the other two periods. This can be seen by looking at the maximum value of $\bar{Q}$ in the center of the gyre; in 1955–58 and 1963–68 the 800 isopleth covers a large area that shrinks nearly to zero in 1959–62.

To be more quantitative about this difference, the maximum baroclinic transport of the gyre for these time periods is computed in Table III using the maximum value of $\bar{Q}$ at the center of the gyre. The results indicate that the differences in maximum transport are significant, the maximum range of variability being $\pm 10\%$ of the long-term mean. This is almost half as large as that (i,e., $\pm 25\%$) computed from the transport section displayed in Fig. 3, although this latest calculation (in Table 3) averages over three or more years. The true maximum range of variability of the annual data about the long term mean lies somewhere between $\pm 10\%$ and $\pm 25\%$.

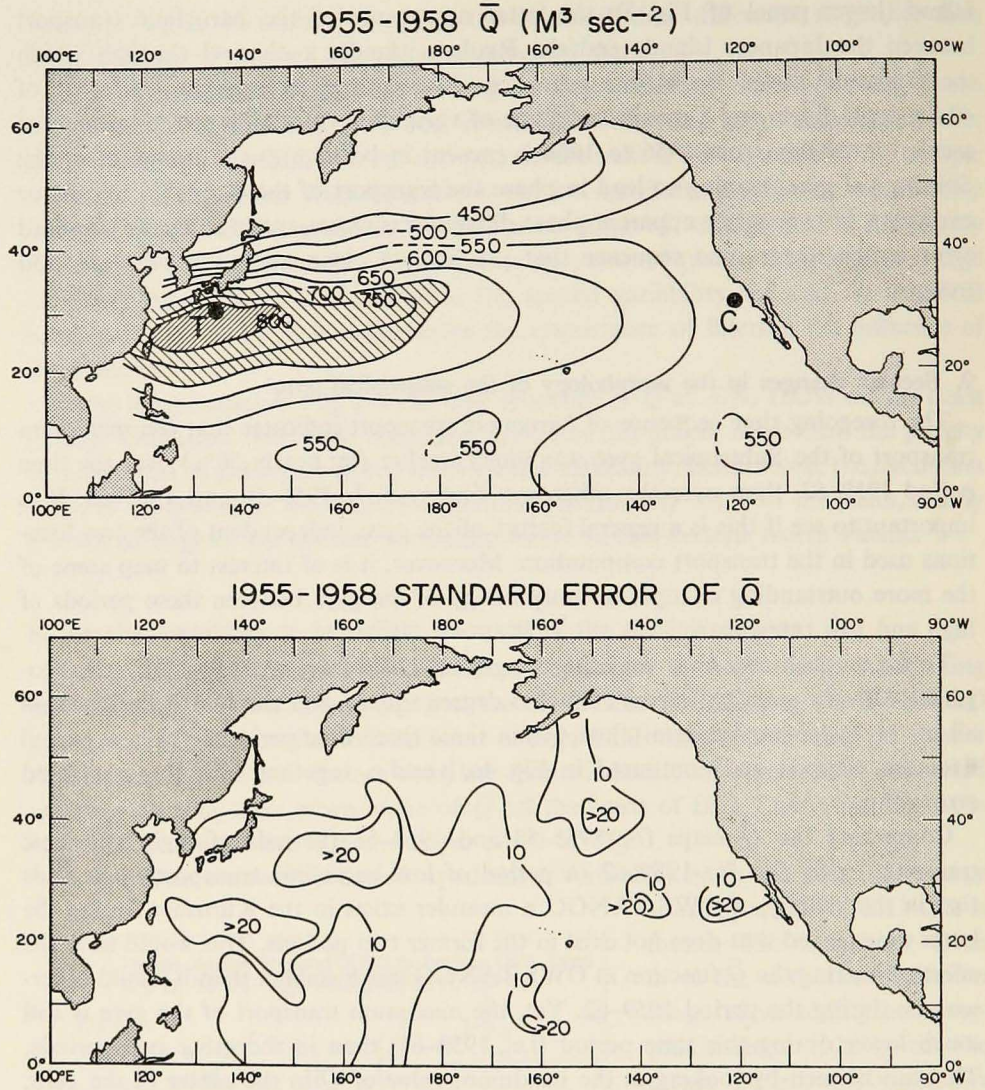

Figure 4 a

Figure 4. Map of the average transport function (Q) and standard error for three time periods: (a) 1955–58, (b) 1959–62, (c) 1963–68. Data from all seasons have been used – dashed lines on the maps indicate where data were absent.

Some other outstanding changes in the shape of the gyre can be seen. During the period of years corresponding to low maximum transport (i.e., 1959–62), the southwest portion of the gyre seems to have extended farther south than it does when the transport is large. On the other hand, the eastward extensions of the gyre in the interior ocean did not seem to change significantly.

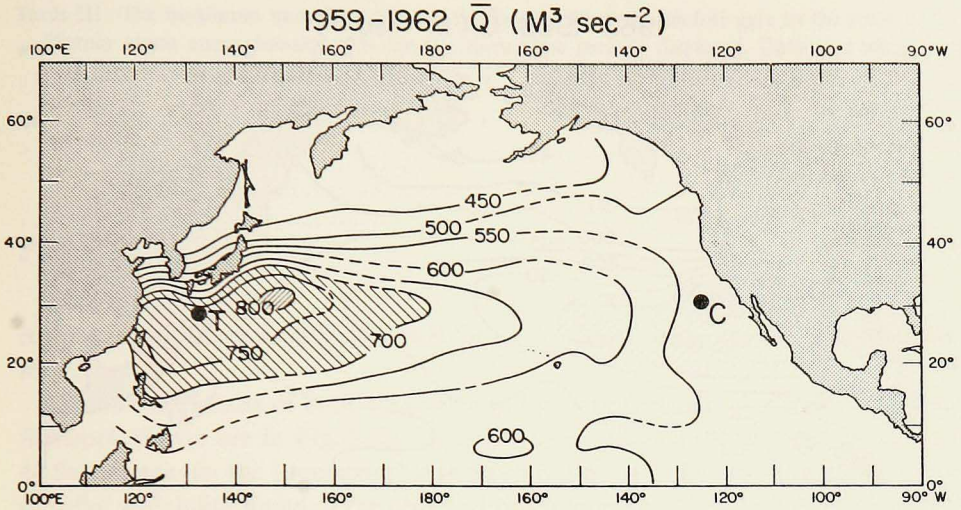

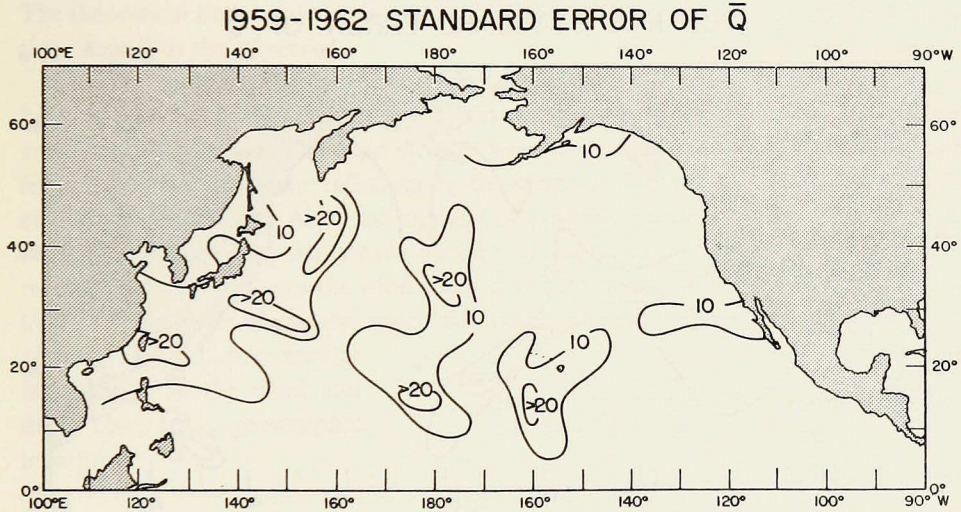

Figure 4 b

10. Comparison of the observed transport variability with that of the Fofonoff/Wickett transport calculations

In this section, the variability of the large-scale baroclinic transport over the interior North Pacific is tested in a simple way against wind driven circulation theory. Although, in general this theory is time-dependent, a time sequence of annual values of geostrophic transport computed from steady state Sverdrup (1947) theory should show secular fluctuations as displayed in the observed time sequence (Fig. 3). This is expected because the observed secular fluctuations have a dominant time scale

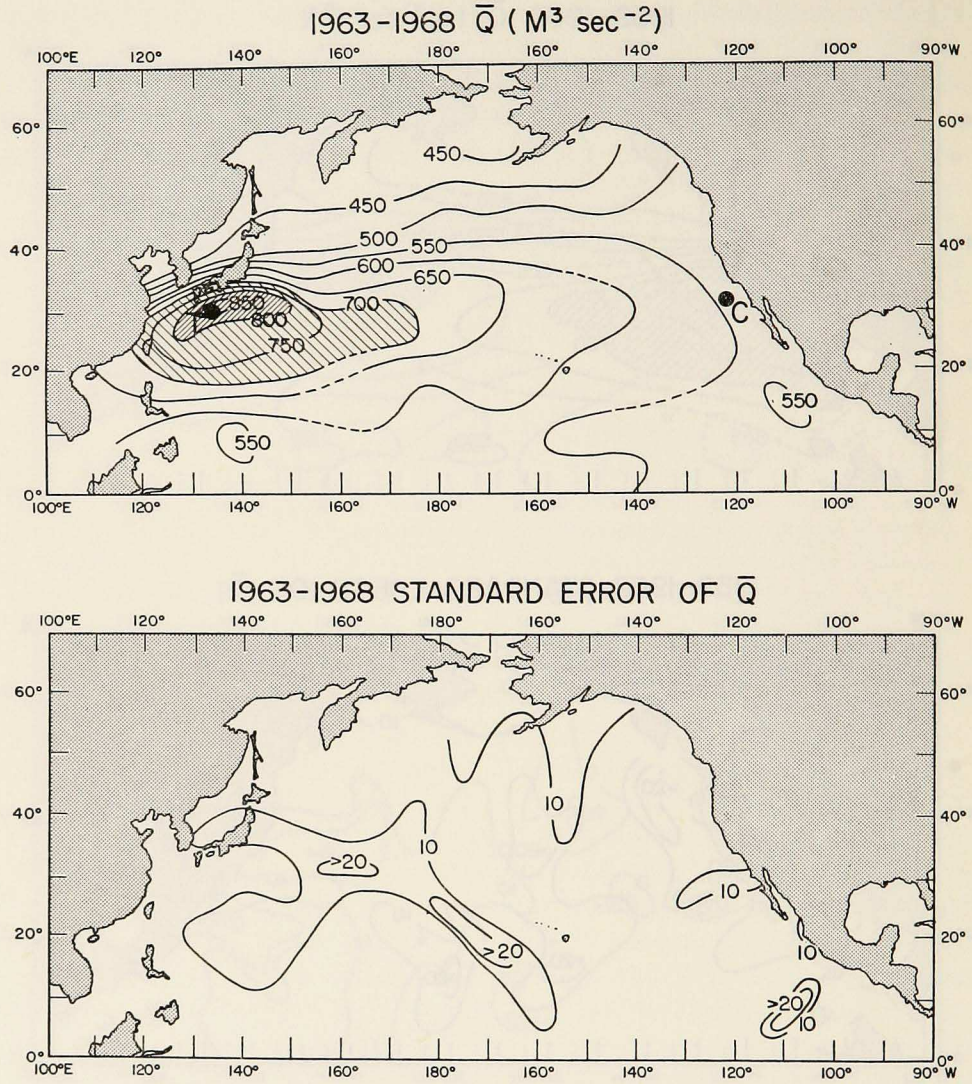

Figure 4 c

(determined by autocorrelation analysis) of 6 years from 1950–70, that is comparable to baroclinic response time predicted for the time-variable wind driven ocean (Veronis and Stommel, 1956) of the same zonal scale length as the North Pacific.

Values of theoretical integrated geostrophic transport have been routinely computed by Fofonoff (1963) and Wickett (1971) over the North Pacific for the twenty year period of interest. The wind stress values were computed from the velocity squared drag law, using monthly mean sea level pressure data to compute the geo-

Table III. The maximum baroclinic transport computed from the central gyre to the coast of California along approximately 30N for the three time periods displayed. Data was taken from data used to contour Figs. 4a, b, c.

Time Period	Maximum Baroclinic Transport *
1955–58	45 *Sv* ± 1 *Sv*
1959–62	37 *Sv* ± 3 *Sv*
1963–68	44 *Sv* ± 1 *Sv*

* Relative to 1000 db.

strophic wind, subsequently corrected for its proximity to the atmospheric boundary layer.

The time sequences of both observed and theoretical geostrophic transport for the Subtropical gyre are in Fig. 5. In the upper panel, the long-term mean transport is 40 Sv, whereas in the lower panel it is much lower, ~ 15 Sv. Moreover, the ±25% range of variability found in the observed time sequence is twice the theoretical, with absolutely no correlation between the two time sequences at periods of about 6 years. The theoretical time sequence is essentially flat compared to the large secular fluctuations found in the observed.

The disagreement between theory and observation may indicate that the theory has not been properly applied, but it may also be that the wind stress distributions are not representative. The wind stresses were computed from monthly mean winds, leaving out the nonlinear influence of the synoptic fluctuations, the latter possibly as large as the former. Also, the analysis of synoptic pressure maps tend to smooth out gradients that may really exist because of the lack of sufficient data coverage to resolve them; this reduces the wind stress curl upon which the theoretical geostrophic transport is based. Certainly, much additional work is required to understand the relationship between secular fluctuations in the wind and the observed geostrophic transport.

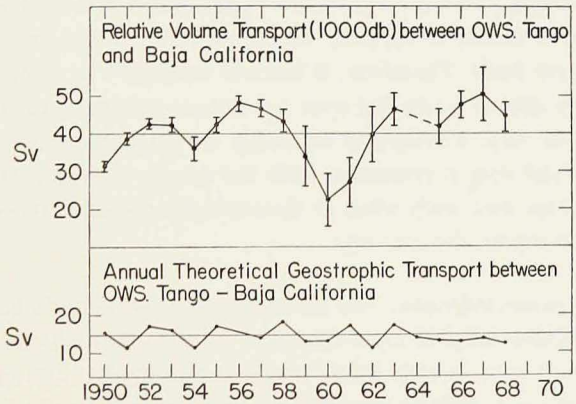

Figure 5. Time sequence of meridional baroclinic transport of the Subtropical gyre (repeated from Fig. 3) and the theoretical geostrophic transport across the same section.

11. Conclusion

A twenty year time sequence of baroclinic transport (0/1000 db) across the Subtropical gyre of the Nnrth Pacific has been constructed from historical hydrographic data obtained from the National Oceanographic Data Center. This time sequence extends

from 1950–1970 and displays significant secular variability, reaching a maximum of approximately ±25% of the long-term mean, with a principal time scale of approximately 6 years. The transport is higher than normal for the years 1955–58 and 1963–68, lower than normal from 1959–62. A comparison of the transpnrt time sequence of the Subtropical gyre with that of the Kuroshio (Nitani, 1972) shows good correlation, with the latter leading the former possibly by one or two years.

In order to investigate how the Subtropical gyre of the North Pacific has altered its morphology during the time periods 1955–58, 1959–62, 1963–68, average maps of the transport function over the North Pacific were constructed. These show a general weakening of the gyre in the western North Pacific during the period 1959–62, associated with the development of a meander in the Kuroshio south of Japan. Also, the southwest portion of the gyre seemed to extend farther south during this time period. On the other hand, the eastern portion of the gyre changed little over these three time periods.

The six year principle time scale of transport variability from 1950–1970 is of the same order as that for a significant baroclinic response of a two-layer ocean to transient large-scale wind systems (Veronis and Stommel, 1956). Therefore, the observed time sequences are compared with time sequences of annual theoretical geostrophic transport across the same section, taken from the work of Fofonoff (1963) and Wickett (1971). These latter calculations were made using geostrophic winds obtained from the monthly mean sea level pressure maps. Between the observed and theoretical time sequences no correlation exists, the theoretical time sequence being essentially flat. Reasons for this disagreement may be due to misapplication of the theory, but equally likely a more representative set of wind data needs to be used; as yet, no other is in existence.

In computing the observed large-scale transport, the presence of the local baroclinic eddy field presented a serious space/time aliasing problem. The baroclinic eddies in the central North Pacific has a principal wave length of 500 km (Bernstein and White, 1974), with transports on the same order as that of the entire Subtropical gyre itself. Therefore, it became necessary to filter out the influence of these eddies by spatial averaging over a 5 degree square at each end of the transport section. In this way, a relatively smoothly varying time sequence of transport was obtained, a result that is consistent with the results of Nitani (1972) on how the Kuroshio fluctuates and with what is theoretically thought about how the large-scale baroclinic transport should vary.

Acknowledgment. The materials used in this study have been provided by the National Oceanographic Data Center. I want to thank Tony Tubbs for arranging these materials in a useable format here at Scripps Institution, and Ted Walker for aid in the analysis of these materials. In particular, I would like to express my appreciation to Robert Bernstein for the many discussions that led to understanding of how the baroclinic eddy field aliased the initial time sequences of large-scale transport.

This research was sponsored by the National Science Foundation and the Office of Naval Research under the Office of Naval Research contract Number N000-14-69-A-0200-6043, and the University of California San Diego, Scripps Institution of Oceanography through NORPAX.

REFERENCES

Bernstein, R. L., and W. B. White. 1974. Time and length scales of baroclinic eddies in the central North Pacific Ocean, (in press) J. Phys. Oceanogr: *4*(4): 613–624.

Fofonoff, N. P. and collaborators. 1963. Transport computations for the North Pacific (*and previously routinely prepared volumes*). Fish. Res. Brd. of Canada, Manuscript Rep. Series # 149–153, # 77–80, # 85, # 128, # 164.

Namias, J. 1968. Long range weather forecasting-history, current status, and outlook. Bull. Am. Met. Soc., *49*(5): 438–470.

Nitani, H. 1972. Beginning of the Kuroshio. *In* Kuroshio, Physical Aspects of the Japan Current. Univ. of Washington Press, Seattle: 517 pp.

Reid, J. 1961. On the geostrophic flow at the surface of the Pacific Ocean with respect to the 1000-decibar surface. Tellus, *13*(4): 489–502.

Sverdrup, H. U. 1947. Wind-driven currents in a baroclinic ocean: with application to the equatorial currents of the eastern Pacific. Proc. Nat',. Acad. Sci. U.S., *33*: 318–326.

Veronis, G. and H. Stommel. 1956. The action of variable wind stress on a stratified ocean. J. Mar. Res., *15*(1): 43–75.

Vondar Harr, T., and A. Oort. 1973. New estimate of annual poleward energy transport by northern hemisphere oceans. J. Phys. Oceanogr., *3*(2): 169–172.

Wickett, W. P. 1971. Fofonoff transport computations for the North Pacific Ocean (*and previously routinely prepared volumes*). Fish. Res. Bd. of Canada, Manuscript Rep. Series *å* 53, *å* 126, *å* 238.

Wooster, W., and B. A. Taft. 1958. On the reliability of field measurements of temperature and salinity in the ocean. J. Mar. Res., *17*: 552–566.

Wyrtki, K. 1966. The average annual heat budget of the North Pacific Ocean and its relation to ocean circulation. J. Geophys. Res., *70*(18): 4547–4559.

Received: *23 August, 1973*; revised *28 February, 1974.*